Single-particle cryo-EM of the ryanodine receptor channel in an aqueous environment

Mariah R. Baker, Guizhen Fan and Irina I. Serysheva

Department of Biochemistry and Molecular Biology, The University of Texas Medical School at Houston, 6431 Fannin Street, Houston, TX 77030, USA

Abstract

Ryanodine receptors (RyRs) are tetrameric ligand-gated Ca^{2+} release channels that are responsible for the increase of cytosolic Ca^{2+} concentration leading to muscle contraction. Our current understanding of RyR channel gating and regulation is greatly limited due to the lack of a high-resolution structure of the channel protein. The enormous size and unwieldy shape of Ca^{2+} release channels make X-ray or NMR methods difficult to apply for high-resolution structural analysis of the full-length functional channel. Single-particle electron cryo-microscopy (cryo-EM) is one of the only effective techniques for the study of such a large integral membrane protein and its molecular interactions. Despite recent developments in cryo-EM technologies and break-through single-particle cryo-EM studies of ion channels, cryospecimen preparation, particularly the presence of detergent in the buffer, remains the main impediment to obtaining atomic-resolution structures of ion channels and a multitude of other integral membrane protein complexes. In this review we will discuss properties of several detergents that have been successfully utilized in cryo-EM studies of ion channels and the emergence of the detergent alternative amphipol to stabilize ion channels for structure-function characterization. Future structural studies of challenging specimen like ion channels are likely to be facilitated by cryo-EM amenable detergents or alternative surfactants.

Key Words: Ryanodine receptor, Membrane proteins, Electron cryo-microscopy, Cryospecimen preparation, Detergents, Amphipol

Eur J Transl Myol - Basic Appl Myol 2015; 25 (1): 35-48

Membrane proteins have always been attractive, yet challenging subjects in structural biology. Membrane proteins contain specialized domains that are specifically adapted to reside within the hydrophobic environment of the lipid bilayer allowing for the protein to communicate cell signals across the biological membrane. Ion channels are integral membrane proteins that are responsible for movements of ions across the cell membrane and for maintaining the ion concentration gradients within cells, driving numerous physiological processes such as muscle contraction, fertilization, learning and memory. Given the significant role of ion channels in myriad cell functions, knowledge of their high-resolution 3D structures is a critical prerequisite to our understanding of channel functions and molecular mechanisms underlying membrane transport in both normal and disease states.

While membrane proteins are abundant, representing 20-30% of the proteome, high-resolution structures solved for them are disproportionally less, ~2% of unique proteins in the PDB to date, proving them to be more difficult targets than soluble proteins.[1] Hindering efforts to uncover the structures of ion channels is their association with the lipid bilayer, the need to extract them from the membrane, their unwieldy size and often dynamic nature. Large protein size, flexibility and membrane-associated domains make X-ray crystallography or NMR methods difficult to apply for structure determination of full-length membrane proteins. To date, single-particle electron cryo-microscopy (cryo-EM) has emerged as an effective and straightforward approach for the study of membrane protein complexes, their interactions and dynamics in different functional states in a vitrified aqueous solution or lipid environment.[2-5]

Recent advances in cryo-EM technology in combination with continuing developments in image processing software have made it possible to obtain structures of protein complexes beyond 5 Å resolution, with some achieving near-atomic resolutions of 3-4 Å,

allowing for high-resolution structural models to be derived *de novo* from cryo-EM density maps.[6-14] Applications of these enhanced technologies by single-particle cryo-EM include protein assemblies within a wide range of molecular weights (~170 kDa – ~4 MDa) and complex symmetry.[14-16] Among recently reported near-atomic resolution structures are a 3.4 Å-resolution structure of the tetrameric TRPV1 ion channel and a 4.5 Å-structure of the γ-secretase, a ~170 kDa` membrane-embedded protease, determined by single-particle cryo-EM.[13,14]

The ryanodine receptor (RyR), a homo-tetrameric Ca^{2+} release channel, was one of the first non-icosahedral proteins to be solved by single-particle cryo-EM, in part owing to its massive size of 2.3 MDa. However, despite rigorous efforts spent to investigate structure-functional characteristics of RyR channels, there are major gaps in our knowledge about the structure of these ion channels, their ion-conducting pore and modulator-binding sites, largely due to the lack of atomic-level structural details for the entire channel assembly. Several low- to moderate-resolution structures of the full-length channel have been solved and some functional regions mapped to the 3D structure. In addition, atomic models of small soluble portions of the channel have also been determined by X-ray crystallography representing ~10% of the entire protein.

Among the obstacles for achieving a high-resolution structure of RyR channels are its inherent flexibility and location within the biological membrane. RyR ion channels can be conceptualized as integral membrane scaffolding protein assemblies that function in tight association with a large array of multiple intracellular modulatory proteins/ligands, interacting with the channel complex in a dynamic manner to provide specific functional feedback. Thus, obtaining biochemically homogeneous and functionally stable channel protein from its native source (*i.e.* muscle cell) suitable for structure determination by single-particle cryo-EM, remains one of the major challenges in pursuit of a high-resolution structure of the entire RyR channel. Detergents are traditionally used to make membrane proteins water soluble and suitable for X-ray crystallography, NMR or cryo-EM. However, detergents tend to destabilize and inactivate membrane proteins.[17] While single-particle cryo-EM remains the most viable methodology for structural analysis of large membrane protein complexes such as RyRs, the presence of detergent in the buffer is an impediment to producing high-resolution cryo-EM structures of membrane proteins. This review will focus on the structure determination of the Ca^{2+} release channel by single-particle cryo-EM with an emphasis on cryospecimen preparation. We will discuss how the choice of surfactant may affect cryospecimen preparation and the success of cryo-EM imaging of membrane proteins.

Ryanodine Receptor Biology – From Discovery to Structure

The ryanodine receptor is an intracellular Ca^{2+} release channel that resides in the sarcoplasmic reticulum (SR) membrane and is integral to the Ca^{2+} dependent signaling process of muscle contraction. In skeletal muscle, type 1 RyR (RyR1) forms a macromolecular complex with voltage-gated Ca^{2+} channels, $Ca_V1.1$, located in the adjacent T-tubule membrane, whereby $Ca_V1.1$ senses membrane depolarization and transmits a mechanical signal to RyR1 resulting in the release of Ca^{2+} ions from SR stores through RyR1. The voltage-mediated rapid release of Ca^{2+} into the cytosol from SR stores allows for the contractile apparatus to operate, a process called excitation-contraction coupling. Excitation-contraction coupling in cardiac muscle differs in that the voltage sensor is not physically coupled to the Ca^{2+} release channel, instead, coupling relies upon Ca^{2+} entry through the $Ca_V1.2$ channel to initiate type 2 RyR (RyR2) openings. Disruption of excitation-contraction coupling can result in several pathological consequences. Mice lacking RyR1 or RyR2 protein expression die either prenatally or perinatal.[18,19] Mutations in the RyR channel protein can cause abnormal Ca^{2+} handling and lead to several conditions in humans including Malignant Hyperthermia, Central Core Disease, Multi-minicore Disease, catecholaminergic polymorphic ventricular tachycardia and arrhythmogenic right ventricular cardiomyopathy.[20] Structure-function studies of RyR to date have been conducted in the absence of high-resolution information about the molecular arrangement of the channel, yet this level of information is necessary to understand the molecular basis for excitation-contraction coupling and channel dysfunction.

The RyR channel functions as a homotetrameric channel with a total molecular mass of 2.3 MDa, each monomer containing ~5000 amino acids. The channel consists of a large cytoplasmic N-terminal region (~80% of the protein mass), several membrane-spanning segments and a small cytoplasmic C-terminus. The *N*-terminal domain serves as a scaffold for many regulatory proteins and molecules to bind, including Ca^{2+}, ATP, caffeine, Mg^{2+}, PKA, ryanodine, calmodulin, FK506 binding protein and $Ca_V1.1$. The transmembrane region of RyR contains the ion-conducting pore across the SR membrane, and based on sequence analysis the channel is predicted to contain an even number of membrane spanning helices per subunit, likely between 4 and 12, encompassed within the amino acid sequence 3985-4940.[21-24] However, the exact number of transmembrane helices has yet to be confirmed by direct structural analysis of the channel. Three mammalian isoforms of RyR exist (RyR1-3) and have a relatively high amino acid sequence homology (~65%). Divergent sequences

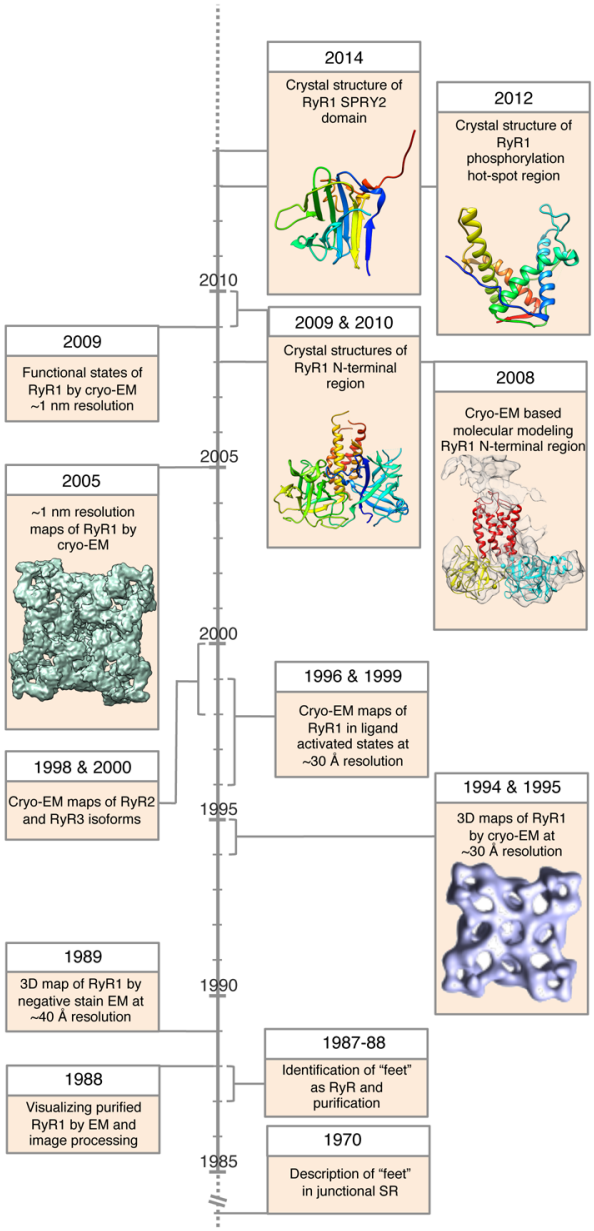

Fig 1. *Timeline summary of RyR1 structural studies.*
RyR1 was first identified as large electron-dense "foot" observed between the junctions of T-tubule and SR membranes.[25] *Over the next two decades many efforts were made to molecularly identify the structure observed in the triad junctions and its role in muscle physiology.*

between the three isoforms occur in domains known as D1 (residues 4254-4631 in RyR1), D2 (residues 1342-1403) and D3 (residues 1872-1923) and are likely responsible for the differences in regulation by the channels. RyR1 is predominantly expressed in skeletal muscle; RyR2 is predominantly expressed in cardiac muscle, and RyR3 is found in brain and diaphragm. None of the isoforms are completely tissue specific, although, RyR1 is the most thoroughly studied isoform due to its abundance in fast-twitch skeletal muscle and relative ease of purification.

The first visual documentation of RyR1 occurred over 40 years ago where RyR1 was identified using thin-section electron microscopy as a large "foot" structure

Eventually, through the use of ^{3}H-ryanodine, differential centrifugation and biophysical characterizations, RyR1 was solidified as the intracellular Ca^{2+} release channel responsible for the release of Ca^{2+} preceding muscle contraction.[27-29] *Due to its relative ease of purification and large size, the structure of RyR1 was investigated by single-particle electron-microscopy. The first 3D structure was obtained by negative stain microscopy, reveling basic morphological features, albeit in a stained and dehydrated state.*[33] *The first depictions of RyR1 in the more native, hydrated conditions came ~4 years later by cryo-EM and were solved to ~30 Å resolution.*[34,36] *Low-resolution structural dynamics of RyR1 gating were described by adding ligands that affect channel open probability to the cryospecimen prior to virtification.*[54,55] *Several additional low-resolution structures of RyR1 were solved that localized small molecule binding sites (CaM, FKBP12 and imperatoxin) and functional domains on the 3D structure of RyR1.*[46,47,50-53] *Structures of RyR2 and RyR3 isoforms were also determined by cryo-EM and appear similar in nature to RyR1.*[43,45] *In two decades since the first structure of RyR1 by cryo-EM was determined, ~1 nm resolution structures were obtained and density based models of channel gating were proposed.*[37,40] *Homology models for the N-terminal domain of the channel were created based on structures of the IP^{3}R1 N-terminus and computationally fitted to the map*[38,39] *Several secondary structure elements in the cytoplasmic and transmembrane domains and subunit boundaries were detectable resulting in a molecular model for some transmembrane helices. Gating induced structural changes were investigated in a ~1 nm resolution structure.*[41] *Structural models for three disease hot-spot domains were determined by X-ray crystallography: the RyR1 N-terminal domain (residues 1-559; PDB: 2XOA), phosphorylation domain (residues 2734-2940; PDB: 4ERT) and SPRY2 domain (residues 1070-1246; PDB: 4P9I, 4P9J, 4P9L).*[59,60,82,98] *With state of the art imaging technology in place, the future for the Ca^{2+} release channel is ripe to proceed towards near-atomic resolutions.*

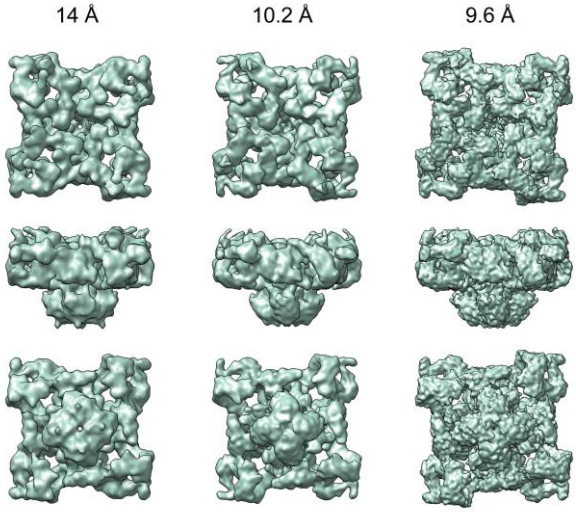

Fig 2. *3D structures of the tetrameric RyR1 channel determined by cryo-EM.*
Surface representations of RyR1 density maps by single-particle cryo-EM viewed in three orthogonal views – from cytoplasm (top), along the membrane plane (middle) and from luminal side (bottom) of the membrane. Left to right are RyR1 density maps at 14 Å (EMD-1274), 10.2 Å (EMD-5014) and 9.6 Å (EMD-1275) resolutions.[37,38,40]

spanning the gap between skeletal muscle T-tubule and SR membranes (Fig. 1).[25] Initially, the composition and role of the foot structure was unclear until biochemical isolation and characterization led to its identification as the Ca^{2+} release channel, which was greatly facilitated by the protein's ability to bind the plant alkaloid ryanodine with high affinity and specificity.[26-31] Early studies on purified single channels by electron microscopy provided a snapshot into the channel ultrastructure and basic quaternary features, followed by the first 3D reconstruction of negatively stained channel particles determined to ~40 Å resolution.[32,33] These studies paved the way for determining the structure of the detergent-solubilized RyR1 under frozen, hydrated conditions by cryo-EM. Extensive efforts have been made to study the 3D structure of the detergent-solubilized RyR1 by using electron microscopy of both single particles[34-41] and 2D crystals.[42]

The first structures of RyR1 by single-particle cryo-EM were generated for the 'closed' Ca^{2+}-depleted state by two different groups to ~40 Å resolution elucidating its now characteristic mushroom-shape appearance[34,36] The general structure of the RyR1 channel exhibits 4-fold symmetry with an overall square-mushroom shape top (280 Å × 280 Å × 120 Å) connected to a stalk structure (120 Å × 120 Å × 60 Å) (Fig 2). Much of RyR1's mass is contained in the cytoplasmic domain and is connected to the transmembrane domain through the stalk structure that is composed of four column domains and rotated ~40° with respect to the cytoplasmic domain. The cytoplasmic region contains several cavities and globular sub-regions with highly flexible clamp-shaped structures present at the corners. Structures of the RyR2 and RyR3 isoforms determined by cryo-EM have an overall architecture similar to that of the RyR1 channel.[43-49] The cytoplasmic portion of RyR1 serves as a scaffold for many of the channel regulators. Several domains[46,47,50] and modulator binding sites (e.g. FKBP12, calmodulin, imperatoxin A have been mapped to the 3D structure of the channel.[51-53] While these structures were determined at low resolutions, they have provided an abundance of information concerning the regulation of the channel. Moreover, in cases where the binding/regulatory sequences are known, localization allows for the assignment of sequence to the 3D structure.

Conformational changes associated with RyR1 channel opening were also addressed by cryo-EM. Based on biochemical and electrophysiological studies, RyR channel gating can be controlled by the presence of Ca^{2+}, adenine nucleotides and ryanodine. The addition of channel activators to the RyR1 cryospecimen permitted samples to be driven into a channel 'open' state, allowing for the investigation of the molecular motions associated with several states of channel gating.[54,55] These studies detailed the first direct evidence of the channel's long-range structural changes under activating conditions revealing general allosteric mass rearrangements that occur with channel gating. At ~30 Å resolution the RyR1 structure exhibited a global conformational change, opening of the cytoplasmic clamp domains, mass depletion and a 4° twist of the transmembrane domain, twisting like the iris of a camera.[54,55]

Our current knowledge of RyR1's structure has progressed from a rather hollow appearing cytoplasmic domain nested atop a dense stalk containing the transmembrane domain to moderately high resolution structures where some secondary structure features are detectable, domain and subunit boundaries are more clearly distinguishable and a putative pore region is described. From the initial data set by Serysheva *et al.*[36] algorithmic improvements in image processing correcting for microscope aberrations using CTF correction resulted in a 14 Å resolution map of RyR1[38] (Fig. 2, left). The improved map exhibited more structural detail and allowed for generation and fitting of a homologous structural model for the RyR1 *N*-terminal domain (residues 216-572) within the clamp region.

The arrangement of α-helices in the transmembrane domain were still ambiguous in the 14 Å resolution density map of RyR1, however, two groups achieving 10.2 Å and 9.6 Å resolution structures (Fig. 2, middle and right) of the Ca^{2+}-depleted state of RyR1 resolved 5-6 α-helices in the transmembrane and pore domains,

including a horizontal helix and a putative pore helix at the luminal side of the channel.[37,39,40] Comparison of the Samso *et al.* structures of the closed and open states indicated that the inner helices kink in order to widen the pore allowing ions to pass through the membrane.[41] Whereas the Ludtke *et al.* structure showed that the inner helices were already kinked in the closed state.[37] Subtle differences in handling the protein, such as freeze-thawing the sample prior to vitrification, cryospecimen preparation or imaging conditions may be at the root of such ambiguity, and higher resolution structures are ultimately necessary to address the transmembrane domain helical arrangement and gating mechanism. Furthermore, modeling of ion permeation pathway of the RyR channels has substantially advanced our understanding of RyR1 gating and ion conduction.[99,100] While these studies are highly important and combine vast research data on RyR function and based primary on available high-resolution crystal structures of the KcsA/KvAP/Shaker channels, they are out of scope of this review and will not be discussed here.

Although all of the previous studies used conventionally accepted methods for resolution determination, currently a more stringent estimation of resolution via the 'gold standard' method has now been adopted by the cryo-EM field making the highest resolution maps currently available for RyR1 more appropriately estimated at ~12-15 Å resolution.[56,57] It is also critical that as cryo-EM produces higher resolution structures that these maps be evaluated for the resolvability of features at the claimed resolution whereby α-helices should appear as rod-like densities at ~9 Å and a helical pitch detectable at ~6-7 Å resolution; β-sheets should appear as planar density at 8-9 Å resolution and strand separation should occur at ~5 Å resolution or better; connectivity between structural features should be identifiable at ~6 Å resolution or better and at ~4 Å resolution bulky side chain densities will begin to appear and the path through the density should be clearly resolved.[57,58]

Prior to any soluble domains of the RyR1 channel solved by X-ray crystallography, bioinformatics and density-constrained comparative modeling were utilized to generate a homology model of the RyR1 N-terminal domain (residues 12–572) based on its high structural homology to the N-terminus of the IP3 receptor, which contains the IP_3 binding and suppressor domains.[39] This model was later confirmed by X-ray crystallography of the RyR1 *N*-terminus. The *N*-terminal structure contains three domains composed of two β-trefoil structures (residues 1–205 and 206–394) followed by a bundle of five α-helices (residues 395–532).[59] While structurally similar to the IP_3 binding domain, RyR1 channel cannot bind or be regulated by IP^3. However, over 30 disease-associated mutations are found in the RyR1 *N*-terminal domain that are proposed to affect channel function by protein misfolding or destabilization of inter- and intra-domain interactions. Fitting of the X-ray structure into the RyR1 cryo-EM density maps yielded two feasible locations, one in the clamp domain and one in the central cytoplasmic vestibule.[39,59]

A structural model of an additional functional domain of the channel was determined by X-ray crystallography for RyR1 residues 2734-2940, which contains 11 disease-associated mutations and a PKA phosphorylation site.[60] The domain is a two-fold symmetrical structure with each half containing two α-helices, one or more short 310 helices and a *C*-terminal β-strand with the halves separated by a long, flexible loop containing the phosphorylation site. This structure was computationally fitted into the clamp domain of the cryo-EM 3D structure of the tetrameric RyR1 channel.[60] However, caution should be used when docking small domains into very large density maps.[61]

At intermediate resolutions (coarser than 1 nm), secondary structure elements are marginally detectable and remain unresolved in a majority of protein densities, resulting in too little structural information to anchor and unambiguously validate fits. In this situation, the validity of the X-ray model fit-to-density is limited by the resolution of the cryo-EM density map and the low resolvability of features in the map can leads to an imperfect match. It is clear that a sufficiently high-resolution cryo-EM map of the full-length channel (<1 nm resolution based on the gold standard criteria), such that secondary structures become better resolved, is required to reconcile the placement of domains and to provide a structural context for RyR1 function. While the current state of the art technology is available for producing near-atomic resolution structures using cryo-EM, cryospecimen preparation is now, more than ever, key to achieving improved resolution density maps for RyR1.

Cryo-EM Imaging of Membrane Proteins in Detergents

Due to recent technical advances in the cryo-EM field, the achievable resolution for membrane proteins is now 3-7 Å,[13,14,62] however vitrification of membrane protein samples is a critical rate-limiting step. In single-particle cryo-EM, the sample is preserved in a layer of vitreous ice and visualized in the form of isolated unordered particles. In general, to achieve a 3D structure using single-particle cryo-EM, the object that is vitrified must be monodisperse in solution and exhibit random orientations. A 3D reconstruction can be obtained through image processing by combining of thousands of 2D projection images of the 3D object being imaged. Integral membrane proteins naturally reside in a lipid bilayer satisfying the hydrophobicity of their transmembrane domain. Thus, to achieve vitrification conditions for cryo-EM visualization, membrane proteins are extracted from their native

membrane environment and imaged in detergent-bound forms in aqueous solution.[17] However, the loss of the structural support provided by the native membrane environment can lead to destabilization and inactivation of membrane proteins, which contributes a significant barrier to membrane protein research in general.[63] Moreover, cryo-EM studies confront the additional hurdle of the presence of detergent in the sample, that can prevent the particles from being distributed evenly in the embedding ice and dramatically reduce the image contrast critical to producing reliable and high-resolution cryo-EM reconstruction.[64]

Single-particle cryo-EM studies of membrane proteins are substantially reliant on the successful solubilization and purification of monodisperse, isotropic solutions of the target protein. Integral membrane proteins exhibit a complex distribution of surface charges where the hydrophobic transmembrane domains are separated by intervening hydrophilic regions that are typically exposed into aqueous intra- or extra-cellular environment. Thus, membrane proteins extracted from their membranous environment will not be water-soluble unless they are placed in a surrounding environment compatible with their hydrophobicity. Due to their amphipathic nature, detergents allow for the removal of membrane proteins from a lipid environment while maintaining their solubility in aqueous solution. Detergents bind to hydrophobic transmembrane domains of membrane proteins and form an amphipathic belt, solubilizing the protein and substituting for the lipid bilayer.[17] These detergent belts are in rapid equilibrium with free detergent monomers and detergent micelles. Thus, the molecular properties and physical behavior of the detergent in the form of micelle and protein-detergent complexes are critical parameters to be considered and controlled in determining the success of single-particle cryo-EM experiments.

The primary difficulty encountered in the single-particle cryo-EM study of detergent-bound membrane proteins is preparation of cryospecimen with particles being evenly distributed within a thin layer of vitreous ice. In general, vitrification of proteins depends on environmental conditions such as temperature, humidity, buffer composition, pH, ionic strength, and surface properties of a supporting film on EM grid. While recent development of semi-automated devices have significantly improved the search for optimal conditions for ice-embedding, the presence of detergent in the membrane protein sample adds to the complexity of the system by changing the surface properties of its components. The presence of detergent in solution reduces the surface tension of the buffer making it difficult to obtain uniform ice film with evenly distributed vitrified particles of membrane protein. Particles that do not adhere to the grid or form a narrow peripheral band close to the edge of the hole in the cryospecimen is a common obstacle in single-particle cryo-EM studies of membrane proteins. This is disadvantageous to cryo-EM data collection since imaging fields often yields only few membrane protein particles per frame. To overcome this difficulty, a continuous carbon film is often used to improve adhering particles to the EM grid (reviewed in[65]). However, in the presence of carbon supporting film, the RyR1 channel particles exhibit a strong preferred orientation with a majority of particles appearing along the four-fold channel axis. While oblique views are certainly present within the cryospecimen and can be retrieved via iterative image processing procedure,[36] their presence is highly variable and specimen dependent. It requires a collection of substantially larger data sets to bring these oblique views to statistical significance in order to achieve reliable isotropic reconstruction of RyR channels.

Another difficulty in cryo-EM study of membrane proteins is that the presence of detergent in the cryospecimen substantially reduces signal to noise ratio in EM images, which is already considered very low for single-particle studies. This effect is particularly disastrous for the high-resolution signal where contrast is marginal even without detergent. For optimal stability of protein-detergent complexes, detergent concentrations are kept near or above the critical micelle-forming concentration (CMC), meaning the buffer is nearly saturated with detergent molecules, which produces a tremendous level of 'noise' in cryo-EM images and can reduce image contrast. This is by far a limiting aspect of cryo-EM visualization of membrane proteins in detergent. This point has not been widely understood in the cryo-EM community since the detergent also produces very strong Thon rings, giving such images an appearance of very good quality when judged by its power spectrum. While there is no accepted standard for assessing a minimal acceptable contrast level in the raw cryo-EM images, it is evident that as contrast is reduced, image processing becomes more susceptible to a model bias and producing a reliable 3D reconstruction becomes problematic.[64]

Clearly, the physical behavior of detergents and properties of protein-detergent complexes must be considered and controlled during cryo-EM experiments. However, despite the increasing number of structures of membrane proteins solved by single-particle cryo-EM, ice-embedding procedure for membrane proteins remains most difficult due to the lack straightforward, reproducible methodologies and strategies. The choice of the detergent chosen for the disruption of lipid bilayer and extraction of the membrane protein of interest is rather more empirical than knowledge-driven procedure. In light of the complexities of protein-detergent interactions, it is important to preserve structure and function of membrane proteins while maintaining their solubility.

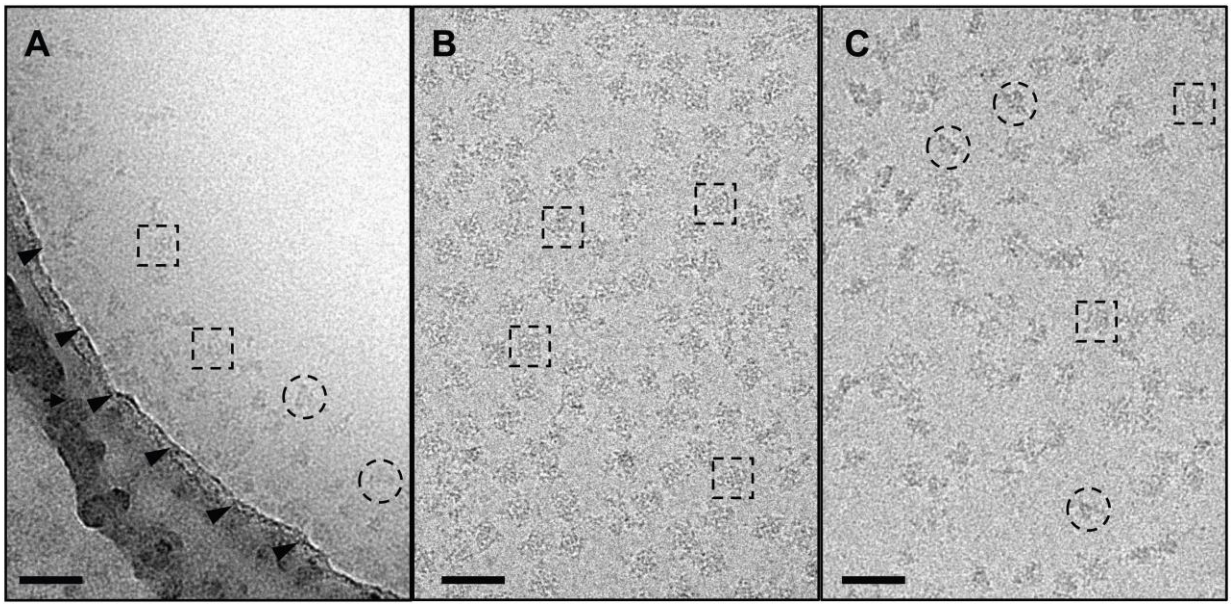

Fig 3. *Cryo-EM images of ice-embedded purified RyR1: in the presence of 0.4 % CHAPS (A) in the presence of A8-35 (B); in the presence of A8-35/n-octyl glucoside [OG]. Note preferred orientation of RyR1 particles in (B), while the particles are randomly oriented within the vitreous ice due to achieved optimal protein/Apol8-35/OG ratio in the cryospecimen shown in (C). Images were recorded on a Gatan 4k x 4k CCD camera using JEM2010F cryomicroscope operated under minimal electron dose conditions (~20 ^{e}-/Å^{2}).*
Scale bars are 500 Å.

However, no 'magic bullet' detergent exists for handling all membrane proteins in a manner suitable for single-particle cryo-EM experiments, and often trial-and-error is the only way to tell. Examples of successful single-particle EM studies of ion channels and some other integral membrane proteins are given in Table 1. Despite the fact that critical information on vitrification of membrane proteins is unpublished, bits of lore can be extracted from these studies to rationalize cryo-EM experiments with membrane proteins. The general conclusion is that detergents with low CMC and high aggregation number are often not compatible with single-particle cryo-EM (Table 2). Through our experiences with membrane proteins and cryo-EM we found that single-particle cryo-EM experiment should be performed at or just below CMC to improve adhesion of membrane protein particles within a layer of vitreous ice on the EM grid yet maintain a soluble membrane protein. Having too little detergent in solution can shift the equilibrium to favor detergent monomers over micelles, leading to unprotected transmembrane domains and protein aggregation while, too much detergent may dissociate some stabilizing lipids required to maintain the protein's structure and affect ice-embedding procedure. Overall, selection of the appropriate detergent for the study of membrane protein by single-particle cryo-EM requires the consideration of how it will impact the protein activity, quaternary structure and its propensity for vitrification. The limited current understanding of protein/detergent systems and forces that maintain the sample in a vitreous ice have frustrated efforts of many researches to exploit the structure of membrane proteins using single-particle cryo-EM and stimulated the developments of approaches to transfer membrane proteins to a more tractable environment that would satisfy the hydrophobic nature of the transmembrane domains and allow for reproducible successful vitrification.[5,66-68] Alternatives to maintaining membrane proteins in non-detergent aqueous solutions, like amphipols, have begun to prove useful in cryo-EM.

Imaging of Membrane Proteins in Detergent-free Aqueous Solution

To circumvent detergent-imposed difficulties in single-particle cryo-EM studies of membrane proteins, amphipols (Apols) have recently been adopted in cryospecimen preparation with much success. Cryo-EM structures of Apol bound TRPV1 channel and γ-secretase complex were solved at 3.4 Å and 4.5 Å, respectively, resolving their transmembrane domains at resolutions where the cryo-EM density maps served as the basis for generating *de novo* molecular structures.[13,14] The use of Apols allows for a detergent-free approach to maintain membrane protein complexes in solution and provides several benefits for attaining high-resolution structures by single-particle cryo-EM.

Table 1. Detergent properties used in single-particle cryo-EM of ion channels. The physical properties of used detergents including CMC, micelle size and molecular weight are important considerations when optimizing cryospecimen conditions.

Detergent	CMC (mM)	CMC (%w/v)	Micelle Size (Da)	Molecular Weight	Aggregation Number
CHAPS 3-[(3-Cholamidopropyl)-dimethyl-ammonio]-1-propanesulfonate	8	0.5	6,150	615	10
Triton X-100 polyethylene glycol p-(1,1,3,3-tetramethylbutyl)-phenyl ether	0.22-0.24	0.01-0.016	90,000	625	100-155
Digitonin	<0.5	0.02	70,000	1,229	60
DDM n-Dodecyl- β-D-maltoside	0.17	0.0087	72,000	511	78-149
DM n-Decyl-β-D-maltopyranosid	1.8	0.087	33,000	483	98
OG n-Octyl-β-D-glucoside	23-25	0.67-0.73	8,000	292	27-100

Apols are a new class of amphipathic polymers that are designed to substitute for detergents, keeping membrane protein complexes soluble and functional in aqueous solution.[69-71] Apols are considered more mild surfactants than detergents and exhibit a very high affinity for transmembrane surfaces due to a large number of hydrophobic chains. Apols interact non-covalently forming a protective belt around the transmembrane domain, and yet they bind almost irreversibly in the absence of detergent (≥ CMC) and have an exceedingly low rate of spontaneous desorption.[72] However, Apols are weak membrane solubilizing surfactants and detergents are still necessary to extract membrane proteins from the lipid membrane. Detergents can easily be exchanged for Apols and removed from solution allowing for the membrane protein to be in a milder detergent-free aqueous environment while preventing protein aggregation and preserving protein structure-function stability.69-71 Membrane proteins are structurally flexible by the very nature of their function, which can often be a detriment to producing a structurally homogenous sample. Apols have been shown to stabilize transmembrane domains and require virtually no excess solution concentration once they have been substituted for detergent.[70,73-75] Based on these favorable properties, Apols are a promising option in the pursuit of membrane protein structures by cryo-EM.

Amphipol 8-35 (A8-35), one of the most well-characterized Apol, appears to be particularly amenable for single-particle cryo-EM studies of ion channels.70 Our group initiated studies of RyR1 in complex with A8-35, a highly water-soluble derivative of polyacrylic acid.[70,76,77] In cryo-EM studies, trapping detergent-solubilized RyR1 with A8-35 allowed reproducibility to vitrify RyR1 channel within the holes of a holey-carbon grids with particles well dispersed throughout the ice (Fig. 3A,B). Our initial studies of the vitrified RyR1/A8-35 complex showed a strongly preferred particle orientation, similar to RyR1 protein frozen on supporting continuous carbon-film. The mechanism behind why RyR1 adopts a preferred orientation in comparison to other membrane proteins, like the IP3R channel, is unknown, however, RyR1's complexity of surface charges combined with its awkward organization in 3D space due to its enormous cytoplasmic domain (>80% of protein mass) likely play a role in driving the preferred orientation. Furthermore, in the presence of A8-35, we believe that the polymer forms a negatively charged film at the water-air interface during sample application to the EM grid resulting in channel particles in a preferred orientation. The addition of octyl-glucoside (OG) in a

Table 2. Attributes of membrane protein complexes determined by single-particle cryo-EM. *A summary of membrane protein structural studies and cryospecimen surfactants used. Listed for each macromolecular complex is the: molecular weight, EMDataBank [EMD] identification number, when available, author's reported resolution (Å) and surfactant type and amount present in cryospecimen.*

Membrane Protein	M.W. (Mda)	EMDB ID	Resolution (Å)	Surfactant and amount reported in cryospecimen			Refs.
				Surfactant	Amt	x CMC	
Intracellular Ca^{2+} Release Channels							
RyR1	2.3	1274	14	CHAPS	0.40%	0.8-1	(38)
		1275	9.6	CHAPS	0.40%	0.8-1	(37)
		5014	10.3	CHAPS	0.50%	1	(40)
		1607, 1606	10.2	CHAPS	0.50%	1	(41)
IP_3R1	1.3	—	24	CHAPS	0.40%	0.8-1	(83)
		—	30	Triton X-100	0.15%	>10	(84)
		5278	10	CHAPS	0.40%	0.8-1	(85)
		1061	20	CHAPS	1%	2	(86)
Voltage Gated Ca^{2+} Channel							
DHPR ($Ca_V1.1$)	0.55	—	25	Digitonin	0.10%	5	(87)
		1069	25	Digitonin	0.10%	5	(88)
Transient Receptor Potential (TRP) Channels							
TRPC3	0.388	—	15	DM	5 mM	2.7	(89)
TRPV4	0.39	—	35	DDM	1 mM	5.9	(90)
TRPV1	0.3	—	19	DM	0.1%	1.15	(91)
TRPV1	0.3	5778	3.27	Apol	1:3 (w/w)	—	(13)
TRPV1	0.3	5776, 5777	3.8 4.2	Apol	1:3 (w/w)	—	(12)
TRPV2	0.36	5688	13.6	decyl-MNG	0.006%	1.8	(92)
TRPA1	0.525	5334	16	A8-35	1:2.3 (w/w)	—	(93)
Other Membrane Proteins							
K_VAP-Fab	0.3	1094	10.5	DM	5mM	2.7	(94)
MCA channel	0.2	2313	26	Ammonium perfluoro-octanoate	4%	3.4	(95)
GluR	0.37	2680 2684 2685 2686 2687 2688 2689	10.4 12.8 7.6 21.4 25.9 22.9 16.4	DDM	0.75 mM	4.4	(62)
γ-Secretase	0.17	2677, 2678	4.5 5.4	A8-35	1:3 (w/w)	—	(14)
ATPase	0.6	5335	9.7	DDM	0.02%	2.3	(96)
	0.9	5476	11	DDM	0.03%	3.4	(97)

concentration 10 times below its CMC resulted in a random distribution of channel particles that we believe is caused by OG disrupting the polymer film (Fig. 3C). Detergents below their CMC remain as monomers in solution and do not disrupt the Apol/membrane protein complex and no significant

loss of signal was observed.[72] Similar approaches for adding small amount of detergent have been used in other imaging projects to reduce preferred orientation.[7] Another approach is the use of short-chain phospholipids, such as DHPC, that are believed to not strongly interact with the membrane protein but can form a monolayer at the air-water interface to reduce surface interactions with the Apol.[78,79] Such monolayers represent a very low volumetric concentration and should not have any significant impact on image contrast.

Increased image contrast in the presence of Apol is particularly critical in the pursuit of high-resolution structures of membrane proteins in general. In cryo-EM images of Apol bound RyR1, the background observed is dramatically lower than in images with detergent present. The Apol bound RyR1 data has ~2-6% contrast at 5-10 Å resolution as compared to 0-2% in the presence of CHAPS using a traditional CCD detector. Advancements in cryo-EM imaging detectors have led to an increased contrast in at high to intermediate resolutions and are one of the reasons the field is seeing an increase of near-atomic resolution structures solved by cryo-EM. With new technology in place, a more stabilized protein with higher image contrast in detergent-free solution will greatly benefit the structural studies of the RyR1 channel complex.

In order to address the structure-function relationship using cryo-EM, it is important that proteins are assessed for their functionality in solution, when possible. We have tested the functionality of RyR1/A8-35 complexes by [^{3}H]-ryanodine binding assay, which yielded a Kd of 1.99 nM and Bmax of 60.4 pmol/mg, similar to that of purified RyR1 in the presence of 0.4% CHAPS (Fig. 4).[80,81] Since, ryanodine binds specifically and with high affinity preferentially to the open state of the intact RyR1 channel, this radioligand binding assay can be considered as an indirect measure of channel activation and indication of its tetrameric structure.[30]

It is evident by recent structural studies by cryo-EM that Apols have a major advantage in stabilizing membrane proteins in aqueous solution, reducing detergent-based background in cryo-imaging and maintaining functionality. Determining the structure of many challenging membrane proteins, like the Ca^{2+} release channel, by cryo-EM will no doubt be well served by detergent alternatives like Apols.

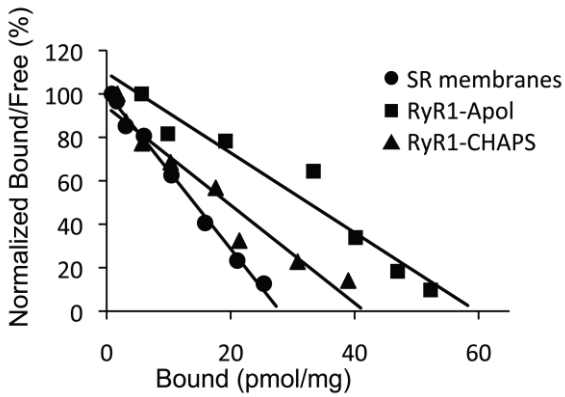

Fig 4. *Scatchard analysis of [^{3}H]-ryanodine binding to RyR1: in skeletal muscle SR membranes (●), purified RyR1 bound to CHAPS (▲) and 800 purified RyR1 in complex with A8-35 (■). Linear fitting yielded Kd of 1.99 nM and Bmax of 60.4 pmol/mg of protein for RyR1/A8-35, and Kd of 41.27 nM and Bmax of 3.07 pmol/mg for RyR1/CHAPS and Kd of 2.54 nM and Bmax of 27.9 pmol/mg for SR membranes in high Ca^{2+} conditions (200μM Ca^{2+}), indicating that the high-affinity binding site for ryanodine is retained in RyR1/Apol and similar to that of RyR1 embedded within the SR membrane.*

Future outlook

While much progress has been made in the elucidation of the structure of RyR1 by cryo-EM and X-ray crystallography, there is still a need to pursue atomic level resolution structures of the channel in order to fully understand channel function. Cryo-EM and image processing technology, with their continuing advancements, are in their prime to be able to produced atomic-level details in density maps that can be directly utilized for *de novo* model building. Cryospecimen preparation, especially for membrane proteins, now appears to be a major bottleneck in the cryo-EM experiment. It is a formidable challenge to produce biochemically homogeneous and structurally stable large membrane protein complexes like the Ca^{2+} release channel and is compounded by the structural flexibility inherent to RyRs complex allosteric regulation. The successful use of detergent alternatives, like Apols, will undoubtedly energize the field of the membrane protein structural biology by cryo-EM. The momentum in single-particle cryo-EM is currently remarkable and near-atomic resolution structures of the entire Ca^{2+} release channel should be expected in near future.

Note added at proof

While this review was in press, three new cryo-EM structures of RyR1 were deposited to EM Data Bank (EMDB ID: 2751, 2752, 6106, 6107 and 2807). The structures were determined at 4.8-8 Å resolutions based on the "gold-standard" criteria.[56]

Acknowledgement

This research is supported by grants from the National Institutes of Health (R01GM072804, R21AR063255, P41RR002250 and S10OD016279), the American Heart Association (14RNT1980029) and the Muscular Dystrophy Association (295138).

Contributions of Authors

MRB, GF and IS prepared the manuscript and performed all work.

Corresponding Author

Irina I. Serysheva, Department of Biochemistry and Molecular Biology, The University of Texas Medical School, 6431 Fannin, MSB 6.219, Houston, TX 77030 U. S. A. Tel.: 713-500-5523, Fax: 713-500-6297
E-mail: irina.i.serysheva@uth.tmc.edu
E-mails of Co-Authors
Mariah R. Baker: mariah.r.Baker@uth.tmc.edu
Guizhen Fan: guizhen.fan@uth.tmc.edu

References

1. Baker ML, Baker MR, Cong Y. Computational Methods for Interpretation of EM Maps at Subnanometer Resolution. eLS. Chichester: JohnWiley&Sons, Ltd; 2012.
2. Cong Y, Ludtke SJ. Single particle analysis at high resolution. Meth Enzymol 2010;482:211-35.
3. Lau WC, Rubinstein JL. Single particle electron microscopy. Methods in molecular biology. 2013;955:401-26.
4. Liao M, Cao E, Julius D, Cheng Y. Single particle electron cryo-microscopy of a mammalian ion channel. Current opinion in structural biology 2014;27C:1-7.
5. Wang L, Sigworth FJ. Structure of the BK potassium channel in a lipid membrane from electron cryomicroscopy. Nature 2009;461(7261):292-5.
6. Cong Y, Baker ML, Jakana J, et al. 4.0- Å resolution cryo-EM structure of the mammalian chaperonin TRiC/CCT reveals its unique subunit arrangement. Proc Natl Acad Sci U S A 2010;107:4967-72.
7. Zhang J, Baker ML, Schroder GF, et al. Mechanism of folding chamber closure in a group II chaperonin. Nature 2010;463(7279):379-83.
8. Zhang X, Settembre E, Xu C, et al. Near-atomic resolution using electron cryomicroscopy and single-particle reconstruction. Proc Natl Acad Sci U S A 2008;105:1867-72.
9. Ludtke SJ, Baker ML, Chen DH, et al. De novo backbone trace of GroEL from single particle electron cryomicroscopy. Structure 2008;16:441-8.
10. Yu X, Jin L, Zhou ZH. 3.88 Å structure of cytoplasmic polyhedrosis virus by cryo-electron microscopy. Nature 2008;453(7193):415-9.
11. Jiang W, Baker ML, Jakana J, et al. Backbone structure of the infectious epsilon15 virus capsid revealed by electron cryomicroscopy. Nature 2008;451(7182):1130-4.
12. Cao E, Liao M, Cheng Y, Julius D. TRPV1 structures in distinct conformations reveal activation mechanisms. Nature 2013;504(7478):113-8.
13. Liao M, Cao E, Julius D, Cheng Y. Structure of the TRPV1 ion channel determined by electron cryo-microscopy. Nature 2013;504(7478):107-12.
14. Lu P, Bai XC, Ma D, Xie T, Yan C, Sun L, et al. Three-dimensional structure of human gamma-secretase. Nature 2014;512(7513):166-70.
15. Bai XC, Fernandez IS, McMullan G, Scheres SH. Ribosome structures to near-atomic resolution from thirty thousand cryo-EM particles. eLife 2013;2:e00461.
16. Li X, Mooney P, Zheng S, et al. Electron counting and beam-induced motion correction enable near-atomic-resolution single-particle cryo-EM. Nat Methods 2013;10:584-90.
17. Linke D. Detergents: an overview. Meth Enzymol 2009;463:603-17.
18. Takeshima H, Komazaki S, Hirose K, et al. Embryonic lethality and abnormal cardiac myocytes in mice lacking ryanodine receptor type 2. Embo J 1998;17:3309-16.
19. Takeshima H, Iino M, Takekura H, et al. Excitation-contraction uncoupling and muscular degeneration in mice lacking functional skeletal muscle ryanodine-receptor gene. Nature 1994;369(6481):556-9.
20. Lanner JT. Ryanodine receptor physiology and its role in disease. Adv Exp Med Biol 2012;740:217-34.
21. Takeshima H, Nishimura S, Matsumoto T, et al. Primary structure and expression from complementary DNA of skeletal muscle ryanodine receptor. Nature 1989;339(6224):439-45.
22. Zorzato F, Fujii J, Otsu K, et al. Molecular cloning of cDNA encoding human and rabbit forms of the Ca^{2+} release channel (ryanodine receptor) of skeletal muscle sarcoplasmic reticulum. J Biol Chem 1990;265:2244-56.
23. Tunwell REA, Lai FA. Ryanodine receptor expression in the kidney and a non-excitable kidney epithelial cell. J Biol Chem 1996;271:29583-8.
24. Du GG, Sandhu B, Khanna VK, et al. Topology of the Ca^{2+} release channel of skeletal muscle sarcoplasmic reticulum (RyR1). Proc Natl Acad Sci U S A 2002;99:16725-30.
25. Ferguson DG, Schwartz H, Franzini-Armstrong C. Subunit structure of junctional feet in triads of skeletal muscle: a freeze-drying, rotary-shadowing study. J Cell Biol 1984;99:173542.

26. Franzini-Armstrong C. Structure of sarcoplasmic reticulum. Federation proceedings 1980;39:2403-9.
27. Campbell KP, Franzini-Armstrong C, Shamoo AE. Further characterization of light and heavy sarcoplasmic reticulum vesicles. Identification of the 'sarcoplasmic reticulum feet' associated with heavy sarcoplasmic reticulum vesicles. Biochim Biophys Acta 1980;602:97-116.
28. Inui M, Saito A, Fleischer S. Purification of the ryanodine receptor and identity with feet structures of junctional terminal cisternae of sarcoplasmic reticulum from fast skeletal muscle. J Biol Chem 1987;262:1740-7.
29. Fleischer S, Ogunbunmi EM, Dixon MC, Fleer EA. Localization of Ca^{2+} release channels with ryanodine in junctional terminal cisternae of sarcoplasmic reticulum of fast skeletal muscle. Proc Natl Acad Sci U S A 1985;82:7256-9.
30. Needleman DH, Hamilton SL. Factors influencing [3H] ryanodine binding to the skeletal muscle Ca^{2+} release channel. Anal biochem 1997;248:173-9.
31. Sutko JL, Kenyon JL. Actions of ryanodine [letter]. J Gen Physiol 1990;96:439-45.
32. Saito A, Inui M, Radermacher M, Frank J, Fleischer S. Ultrastructure of the calcium release channel of sarcoplasmic reticulum. J Cell Biol 1988;107:211-9.
33. Wagenknecht T, Grassucci R, Frank J, et al. Three-dimensional architecture of the calcium channel/foot structure of sarcoplasmic reticulum. Nature 1989;338(6211):167-70.
34. Radermacher M, Rao V, Grassucci R, et al. Cryo-electron microscopy and three-dimensional reconstruction of the calcium release channel/ryanodine receptor from skeletal muscle. J Cell Biol 1994;127:411-23.
35. Wagenknecht T, Radermacher M. Three-dimensional architecture of the skeletal muscle ryanodine receptor. FEBS Lett 1995;369:43-6.
36. Serysheva II, Orlova EV, Chiu W, et al. Electron cryomicroscopy and angular reconstitution used to visualize the skeletal muscle calcium release channel. Nat Struct Biol 1995;2:18-24.
37. Ludtke SJ, Serysheva, II, Hamilton SL, Chiu W. The pore structure of the closed RyR1 channel. Structure (Camb) 2005;13:1203-11.
38. Serysheva II, Hamilton SL, Chiu W, Ludtke SJ. Structure of Ca^{2+} release channel at 14 Å resolution. J Mol Biol 2005;345:427-31.
39. Serysheva II, Ludtke SJ, Baker ML, et al. Subnanometer-resolution electron cryomicroscopy-based domain models for the cytoplasmic region of skeletal muscle RyR channel. Proc Natl Acad Sci U S A 2008;105:9610-5.
40. Samso M, Wagenknecht T, Allen PD. Internal structure and visualization of transmembrane domains of the RyR1 calcium release channel by cryo-EM. Nat Struct Mol Biol 2005;12:539-44.
41. Samso M, Feng W, Pessah IN, Allen PD. Coordinated movement of cytoplasmic and transmembrane domains of RyR1 upon gating. PLoS biology 2009;7:e85.
42. Yin CC, Han H, Wei R, Lai FA. Two-dimensional crystallization of the ryanodine receptor Ca^{2+} release channel on lipid membranes. J Struct Biol 2005;149:219-24.
43. Sharma MR, Jeyakumar LH, Fleischer S, Wagenknecht T. Three-dimensional structure of ryanodine receptor isoform three in two conformational states as visualized by cryo-electron microscopy. J Biol Chem 2000;275:9485-91.
44. Liu Z, Zhang J, Sharma MR, et al. Three-dimensional reconstruction of the recombinant type 3 ryanodine receptor and localization of its amino terminus. Proc Natl Acad Sci U S A 2001;98:6104-9.
45. Sharma MR, Penczek P, Grassucci R, et al. Cryoelectron microscopy and image analysis of the cardiac ryanodine receptor. J Biol Chem 1998;273:18429-34.
46. Liu Z, Zhang J, Li P, et al. Three-dimensional reconstruction of the recombinant type 2 ryanodine receptor and localization of its divergent region 1. J Biol Chem 2002;277:46712-9.
47. Zhang J, Liu Z, Masumiya H, et al. Three-dimensional localization of divergent region 3 of the ryanodine receptor to the clamp-shaped structures adjacent to the FKBP binding sites. J Biol Chem 2003;278:14211-8.
48. Liu Z, Wang R, Zhang J, et al. Localization of a disease-associated mutation site in the three-dimensional structure of the cardiac muscle ryanodine receptor. J Biol Chem 2005;280:37941-7.
49. Wang R, Chen W, Cai S, et al. Localization of an NH(2)-terminal disease-causing mutation hot spot to the "clamp" region in the three-dimensional structure of the cardiac ryanodine receptor. J Biol Chem 2007;282:17785-93.
50. Liu Z, Zhang J, Wang R, et al. Location of divergent region 2 on the three-dimensional structure of cardiac muscle ryanodine receptor/calcium release channel. J Mol Biol 2004;338:533-45.
51. Wagenknecht T, Grassucci R, Berkowitz J, et al. Cryoelectron microscopy resolves FK506-binding protein sites on the skeletal muscle ryanodine receptor. Biophys J 1996;70:1709-15.
52. Wagenknecht T, Berkowitz J, Grassucci R, et al. Localization of calmodulin binding sites on the ryanodine receptor from skeletal muscle by electron microscopy. Biophys J 1994;67:2286-95.

53. Samso M, Trujilo R, Gurrola GB, et al. Three-dimensional Location of the Imperatoxin A Binding Site on the Ryanodine Receptor. J Cell Biol 1999;146:493-99.
54. Orlova EV, Serysheva, II, van Heel M, et al.. Two structural configurations of the skeletal muscle calcium release channel. Nat Struct Biol 1996;3:547-52.
55. Serysheva II, Schatz M, van Heel M, et al. Structure of the Skeletal Muscle Calcium Release Channel activated with Ca^{2+} and AMP-PCP. Biophys J 1999;77:1936 - 44.
56. Scheres SH, Chen S. Prevention of overfitting in cryo-EM structure determination. Nat Methods 2012;9(9):853-4.
57. Henderson R, Sali A, Baker ML, et al. Outcome of the first electron microscopy validation task force meeting. Structure 2012;20:205-14.
58. Baker ML, Baker MR, Hryc CF, Dimaio F. Analyses of subnanometer resolution cryo-EM density maps. Meth Enzymol 2010;483:1-29.
59. Tung CC, Lobo PA, Kimlicka L, Van Petegem F. The amino-terminal disease hotspot of ryanodine receptors forms a cytoplasmic vestibule. Nature 2010;468(7323):585-8.
60. Yuchi Z, Lau K, Van Petegem F. Disease mutations in the ryanodine receptor central region: crystal structures of a phosphorylation hot spot domain. Structure 2012;20:1201-11.
61. Egelman EH. Problems in fitting high resolution structures into electron microscopic reconstructions. HFSP J 2008;2:324-31.
62. Meyerson JR, Kumar J, Chittori S, et al. Structural mechanism of glutamate receptor activation and desensitization. Nature 2014;514(7522):328-34.
63. Seddon AM, Curnow P, Booth PJ. Membrane proteins, lipids and detergents: not just a soap opera. Biochim Biophys Acta. 2004;1666:105-17.
64. Stewart A, Grigorieff N. Noise bias in the refinement of structures derived from single particles. Ultramicroscopy 2004;102:67-84.
65. Serysheva, II, Chiu W, Ludtke SJ. Single-particle electron cryomicroscopy of the ion channels in the excitation-contraction coupling junction. Methods Cell Biol 2007;79:407-35.
66. Cheung M, Kajimura N, Makino F, et al. A method to achieve homogeneous dispersion of large transmembrane complexes within the holes of carbon films for electron cryomicroscopy. J Struct Biol 2013;182:51-6.
67. Kelly DF, Dukovski D, Walz T. Strategy for the use of affinity grids to prepare non-His-tagged macromolecular complexes for single-particle electron microscopy. J Mol Biol 2010;400:675-81.
68. Kastner B, Fischer N, Golas MM, et al. GraFix: sample preparation for single-particle electron cryomicroscopy. Nat Methods 2008;5:53-5.
69. Popot JL. Amphipols, nanodiscs, and fluorinated surfactants: three nonconventional approaches to studying membrane proteins in aqueous solutions. Ann Rev Biochem 2010;79:737-75.
70. Tribet C, Audebert R, Popot JL. Amphipols: polymers that keep membrane proteins soluble in aqueous solutions. Proc Natl Acad Sci U S A 1996;93:15047-50.
71. Popot JL, Berry EA, Charvolin D, Creuzenet C, Ebel C, Engelman DM, et al. Amphipols: polymeric surfactants for membrane biology research. Cell Mol Life Sci 2003;60(8):1559-74.
72. Tribet C, Diab C, Dahmane T, et al. Thermodynamic characterization of the exchange of detergents and amphipols at the surfaces of integral membrane proteins. Langmuir 2009;25:12623-34.
73. Champeil P, Menguy T, Tribet C, et al. Interaction of amphipols with sarcoplasmic reticulum Ca^{2+}-ATPase. J Biol Chem 2000;275:18623-37.
74. Picard M, Dahmane T, Garrigos M, et al. Protective and inhibitory effects of various types of amphipols on the Ca^{2+}-ATPase from sarcoplasmic reticulum: a comparative study. Biochemistry 2006;45:1861-9.
75. Pocanschi CL, Dahmane T, Gohon Y, et al. Amphipathic polymers: tools to fold integral membrane proteins to their active form. Biochemistry 2006;45:13954-61.
76. Popova OB, Fan G, Chiu W, et al. Cryo-EM Studies of RyR1 Channel in Detergent-Free Aqueous Environment. Biophys J 2014;106:109.
77. Fan G, Gonzalez J, Popova OB, et al. A first look into the 3D structure of the TRPV2 channel by single-particle cryo-EM. Biophys J 2014;106:600a-1a.
78. Hauser H. Short-chain phospholipids as detergents. Biochim Biophys Acta 2000;1508:164-81.
79. Kessi J, Poiree JC, Wehrli E, et al Short-chain phosphatidylcholines as superior detergents in solubilizing membrane proteins and preserving biological activity. Biochemistry 1994;33:10825-36.
80. Wang JP, Needleman DH, Hamilton SL. Relationship of low affinity [3]ryanodine binding sites to high affinity sites on the skeletal muscle Ca^{2+} release channel. J Biol Chem 1993;268:20974-82.
81. Callaway C, Seryshev A, Wang JP, et al. Localization of the high and low affinity [3H]ryanodine binding sites on the skeletal muscle Ca^{2+} release channel. J Biol Chem 1994;269:15876-84.

82. Lobo PA, Van Petegem F. Crystal structures of the N-terminal domains of cardiac and skeletal muscle ryanodine receptors: insights into disease mutations. Structure 2009;17:1505-14.
83. Jiang QX, Thrower EC, Chester DW, et al. Three-dimensional structure of the type 1 inositol 1,4,5-trisphosphate receptor at 24 Å resolution. Embo J 2002;21:3575-81.
84. Serysheva, II, Bare DJ, Ludtke SJ, et al. Structure of the type 1 inositol 1,4,5-trisphosphate receptor revealed by electron cryomicroscopy. J Biol Chem 2003;278:21319-22.
85. Ludtke SJ, Tran TP, Ngo QT, et al. Flexible architecture of IP^3R1 by Cryo-EM. Structure 2011;19:1192-9.
86. Sato C, Hamada K, Ogura T, et al. Inositol 1,4,5-trisphosphate receptor contains multiple cavities and L-shaped ligand-binding domains. J Mol Biol 2004;336:155-64.
87. Serysheva II, Ludtke SJ, Baker MR, et al. Structure of the voltage-gated L-type Ca2+ channel by electron cryomicroscopy. Proc Natl Acad Sci U S A 2002;99:10370-5.
88. Wolf M, Eberhart A, Glossmann H, et al. Visualization of the domain structure of an L-type Ca^{2+} channel using electron cryo-microscopy. J Mol Biol 2003;332:171-82.
89. Mio K, Ogura T, Kiyonaka S, et al. The TRPC3 channel has a large internal chamber surrounded by signal sensing antennas. J Mol Biol 2007;367:373-83.
90. Shigematsu H, Sokabe T, Danev R, et al. A 3.5-nm structure of rat TRPV4 cation channel revealed by Zernike phase-contrast cryoelectron microscopy. J Biol Chem 2009;285:11210-8.
91. Moiseenkova-Bell VY, Stanciu LA, et al. Structure of TRPV1 channel revealed by electron cryomicroscopy. Proc Natl Acad Sci U S A 2008;105:7451-5.
92. Huynh KW, Cohen MR, Chakrapani S, et al. Structural insight into the assembly of TRPV channels. Structure 2014;22:260-8.
93. Cvetkov TL, Huynh KW, Cohen MR, Moiseenkova-Bell VY. Molecular architecture and subunit organization of TRPA1 ion channel revealed by electron microscopy. J Biol Chem 2011;286:38168-76.
94. Jiang QX, Wang DN, MacKinnon R. Electron microscopic analysis of KvAP voltage-dependent K^+ channels in an open conformation. Nature 2004;430:806-10.
95. Shigematsu H, Iida K, Nakano M, et al. Structural characterization of the mechanosensitive channel candidate MCA2 from Arabidopsis thaliana. PloS one 2014;9:e87724.
96. Lau WC, Rubinstein JL. Subnanometre-resolution structure of the intact Thermus thermophilus H^+-driven ATP synthase. Nature 2012;481(7380):214-8.
97. Benlekbir S, Bueler SA, Rubinstein JL. Structure of the vacuolar-type ATPase from Saccharomyces cerevisiae at 11- Å resolution. Nat Struct Mol Biol 2012;19:1356-62.
98. Lau K, van Petegen F. Crystal structures of wild type and disease mutant forms of the ryanodine receptor SPRY2 domain. Nature Comm 2014;5:5397.
99. Xu L, Wang Y, Gillespie D, Meissner G. Two rings of negative charges in the cytosolic vestibule of type-1 ryanodine receptor modulate ion fluxes. Biophys J 2006;90:443-53.
100. Ramachandran S, Chakraborty A, Xu L, et al.. Structural determinants of skeletal muscle ryanodine receptor. J Biol Chem 2013;288:6154-62.